Received: 11 November 2020 | Revised: 11 February 2021 | Accepted: 1 March 2021

DOI: 10.1096/fj.202002490R

RESEARCH ARTICLE

THE FASEB JOURNAL

Quinomycin A reduces cyst progression in polycystic kidney disease

Priyanka S. Radadiya[1,4] | **Mackenzie M. Thornton**[1,4] | **Emily A. Daniel**[1,4] | **Jessica Y. Idowu**[1,4] | **Wei Wang**[3,4] | **Brenda Magenheimer**[2,4] | **Dharmalingam Subramaniam**[5] | **Pamela V. Tran**[3,4] | **James P. Calvet**[2,4] | **Darren P. Wallace**[1,4] | **Madhulika Sharma**[1]

[1]Departments of Internal Medicine, University of Kansas Medical Center, Kansas City, KS, USA

[2]Biochemistry and Molecular Biology, University of Kansas Medical Center, Kansas City, KS, USA

[3]Anatomy and Cell Biology, University of Kansas Medical Center, Kansas City, KS, USA

[4]The Jared Grantham Kidney Institute, University of Kansas Medical Center, Kansas City, KS, USA

[5]Department of Cancer Biology, University of Kansas Medical Center, Kansas City, KS, USA

Correspondence
Madhulika Sharma, Department of Internal Medicine, University of Kansas Medical Center, Kansas City, KS 66160, USA.
Email: msharma3@kumc.edu

Funding information
This project was supported by an Institutional Development Award (IDeA) from the National Institute of General Medical Sciences of the National Institutes of Health under grant number P20 GM103418-summer scholarship award to PR, PKD Biomarkers, Biomaterials, and Cellular Models Core in the Kansas PKD Research and Translational Core Center (U54 DK126126), which is part of the national PKD Research Resource Consortium; R01DK103033 to PVT, Lied pilot award and R01DK108433 to MS

Abstract

Polycystic kidney disease (PKD) is a genetic disorder characterized by aberrant renal epithelial cell proliferation and formation and progressive growth of numerous fluid-filled cysts within the kidneys. Previously, we showed that there is elevated Notch signaling compared to normal renal epithelial cells and that Notch signaling contributes to the proliferation of cystic cells. Quinomycin A, a bis-intercalator peptide, has previously been shown to target the Notch signaling pathway and inhibit tumor growth in cancer. Here, we show that Quinomycin A decreased cell proliferation and cyst growth of human ADPKD cyst epithelial cells cultured within a 3D collagen gel. Treatment with Quinomycin A reduced kidney weight to body weight ratio and decreased renal cystic area and fibrosis in $Pkd1^{RC/RC}$; $Pkd2^{+/-}$ mice, an orthologous PKD mouse model. This was accompanied by reduced expression of Notch pathway proteins, RBPjk and HeyL and cell proliferation in kidneys of PKD mice. Quinomycin A treatments also normalized cilia length of cyst epithelial cells derived from the collecting ducts. This is the first study to demonstrate that Quinomycin A effectively inhibits PKD progression and suggests that Quinomycin A has potential therapeutic value for PKD patients.

KEYWORDS
Quinomycin A, proliferation, Notch, polycystic kidney

Abbreviations: cAMP, cyclic adenosine monophosphate; DBA, *Dolichos biflorus* agglutinin; EGF, epidermal growth factor; FSK, forskolin; HeyL, hairy/enhancer-of-split related with YRPW motif-like protein; HIF, hypoxia-inducible factor; LTA, *Lotus tetragonolobus* agglutinin; PC1, polycystin 1; PC2, polycystin 2; PKD, polycystic kidney disease; PKHD1, polycystic kidney and hepatic disease 1; RBPjk, recombination signal-binding protein for immunoglobulin kappa J region; SMA, smooth muscle actin.

Priyanka S. Radadiya and Mackenzie M. Thornton contributed equally to the study.

1 | INTRODUCTION

Polycystic kidney disease (PKD) is a genetic disease characterized by formation and expansion of renal cysts resulting from epithelial hyper-proliferation and abnormal cyst-filling fluid secretion.[1,2] Two inherited forms of PKD are: (a) Autosomal dominant polycystic kidney disease (ADPKD), a disease caused by mutations in either *PKD1* or *PKD2*, which encode polycystin-1 (PC1) and polycystin-2 (PC2), respectively, and (b) autosomal recessive polycystic kidney disease (ARPKD), caused by mutations of *PKHD1*, which encodes fibrocystin. PC1, PC2, and fibrocystin form protein complexes that localize to the primary cilium, a non-motile sensory organelle, that transduces mechanical and/or chemical stimuli and mediates cellular signaling.[3]

Several signaling pathways are activated in response to mutations in PC1 and PC2 in ADPKD and efforts are underway to target these pathways. Tolvaptan is presently the only first line treatment approved for ADPKD.[4] Tolvaptan targets the arginine vasopressin receptor AVP V2R leading to decreased cAMP production and inhibition of cell proliferation and cyst growth in ADPKD. However, tolvaptan is poorly tolerated by some patients and can lead to liver complications, demonstrating that there is an unmet need for safer drugs to treat ADPKD.[5] Currently, several drugs shown to have good safety in clinical trials are being evaluated for the treatment of ADPKD, these include metformin, a drug to treat diabetes that acts by inhibiting glycolysis[6]; niacinamide (a form of vitamin B3) that inhibits sirtuin1 and tesevatinib, a tyrosine kinase inhibitor that inhibits epidermal growth factor (EGFR).[7,8]

We previously reported the activation of Notch3 pathway in cystic epithelial cells of various mouse models of PKD as well as renal cystic epithelial cells cultured from human ADPKD patients.[9] The Notch signaling pathway is activated upon binding of a Notch ligand to a Notch receptor, resulting in the gamma secretase-mediated release of the Notch intracellular domain (NICD). The NICD translocates to the nucleus and binds to RBPjk protein and results in transcriptional activation of Notch target genes, *Hes* and *Hey*. Gamma secretase inhibitors (GSI) can inhibit Notch activity in vivo and in vitro, however these inhibitors have been shown to be associated with gastrointestinal toxicity in clinical trials.[10] Thus, we investigated whether repurposing another drug, known to have inhibitory effects on Notch signaling, would attenuate PKD.

Quinomycin A, also called echinomycin is a member of quinoxaline family of antibiotics, originally isolated from Streptomyces echinatus.[11] Quinomycin A can bind strongly to double-stranded DNA and exhibit antitumor activities. Quinomycin A was shown to reduce acute myeloid leukemia in mouse model without any adverse effects on normal hematopoetic cells.[12,13] Quinomycin A also reduced disease progression in a mouse model of pancreatic cancer by targeting the Notch signaling pathway.[14] Thus, we asked whether Quinomycin A can protect against PKD by inhibiting the Notch pathway activation.

Our results show that Quinomycin A inhibits cyst epithelial cell proliferation and cyst growth using both in vitro and in vivo models of PKD. Treatment with Quinomycin A inhibits the activation of the Notch pathway, and reduces cilia lengths of cyst-lining epithelial cells in an ADPKD mouse model. In contrast, Quinomycin A has minimal effects on normal human tubule epithelial cells and normal kidneys of control mice. Taken together, our data demonstrate that Quinomycin A can selectively target PKD cystic epithelial cells.

2 | MATERIALS AND METHODS

2.1 | Antibodies and reagents

Antibodies and their sources are listed: Notch3 and HIF-1α (Abcam), smooth muscle actin (Sigma-Aldrich), RBPjk (Santa Cruz), Hey L (Life Span Biosciences). Ki67 (Dako), anti-acetylated tubulin and Quinomycin A (Sigma-Aldrich), *Dolichos biflorus agglutinin* (DBA), and *Lotus tetragonolobus* agglutinin (LTA) (Vector Laboratories, Inc).

2.2 | Animal care protocols

$Pkd1^{RC/RC}$; $Pkd2^{+/-}$ (PKD) mice were generated by breeding $Pkd1^{RC/RC}$ mice with $Pkd2^{+/-}$ mice (both on a C57BL/6J background) kindly provided by Drs. Peter Harris and Stefen Somlo, respectively.[15,16] Wild-type littermates without a PKD mutation ($Pkd1^{+/+}/Pkd2^{+/+}$) were used as controls. Mice were generated at the PKD Rodent Models and Drug Testing Core at the University of Kansas Medical Center in accordance with the guidelines of the Guide for the Care and Use of Laboratory Animals of the National Institutes of Health (NIH). All the mice used were housed in micro-isolator cages, pathogen-free conditions, on air-filtered, ventilated rack. The protocols used in research were approved by the Institutional Animal Care and Use Committee (IACUC) of the University of Kansas Medical Center (Kansas City, KS).

2.3 | Quinomycin A treatments in mice

Quinomycin A was solubilized in distilled water and sterile-filtered using a 0.2-micron filter for treatments. Study groups consisted of (a) vehicle-treated wild-type (WT) mice, (b) Quinomycin A-treated WT mice, (c) vehicle-treated PKD mice, and (d) Quinomycin A-treated PKD mice. Mice were weaned and treatments were started at P22 for a total of

27 days with daily intraperitoneal injections of 10 μg/kg body weight Quinomycin A. During euthanasia, mice were weighed and perfused with cold PBS after blood collection followed by collecting and weighing kidneys. One kidney was snap frozen and the other was fixed in 4% paraformaldehyde for 24 hours followed by storage in 70% ethanol at 4°C until blocking and sectioning for histology and immunohistochemistry (IHC).

2.4 | Histology, cystic index, and blood urea nitrogen (BUN) measurements

The fixed kidney tissues were processed at the Histology Core at the University of Kansas Medical Center. Five-micrometer sections were stained with hematoxylin and eosin (H&E) as described previously.[17] Cystic index was measured using ImageJ on H&E stained kidney sections. The area of each individual cyst within the section of the entire kidney was calculated to determine the total cyst surface area per section. This summed value was then divided by the total area of the section yielding the value identified as the cystic index. This was done for a kidney section for each mouse used in the study in each PKD group. BUN was quantified using a Quantichrom Urea Assay Kit (Bioassay Systems), according to the manufacturer's protocol.

2.5 | Human cell culture and treatments

Primary cultures of ADPKD and normal human kidney (NHK) cells were generated as described previously.[18] The use of de-identified surgically discarded tissues complies with federal regulations and was approved by the Institutional Review Board at KUMC. ADPKD cells were obtained from multiple surface cysts ranging in size. NHK cells were cultured from sections of cortex. These cells have been shown to be enriched in the collecting duct marker, *Dolichos biflorus agglutinin* (DBA).[19] Cells were cultured in DMEM/F-12 supplemented with 5% of FBS, 5 μg/mL of insulin, 5 μg/mL of transferrin, 5 ng/mL of sodium selenite (ITS, Thermo Scientific), 100 U/mL of penicillin (100 U/mL), and 130 μg/mL of streptomycin.[20] Cultures were not passaged more than twice before being used in experiments. For treatments, ADPKD cells were grown to 70% confluency followed by a 24-hour low serum (0.001% and no ITS) treatment. Cells were then treated with vehicle or Quinomycin A for 4 days before studies.

2.6 | Cell viability assay

ADPKD or NHK cells were plated in a 12-well plate (20,000 cells/well) and allowed to grow to 70% confluency at 37°C under 5% CO_2 followed by 24-hour low serum (0.001%) and no ITS treatment. The following day cells were treated with increasing concentrations of Quinomycin A (0 to 10 nmol/L). Cells were grown for 4 days and fresh medium-containing Quinomycin A was replaced every day. After 4 days, cells were trypsinized and pelleted. Cells were suspended in 500 μL media and cell viability was tested in triplicates using the cell counting kit-8 (CCK-8, Apex Biosciences) according to the manufacturer's instructions. Viability was set at 100% for the vehicle control and relative values were calculated for other doses.

2.7 | In vitro 3D cyst assays

In vitro cyst assays were performed as described.[21-23] Briefly, primary cultures of ADPKD cells were suspended in media containing type 1 collagen (PureCol, Advanced Biomatrix) in a 96-well plate. Immediately after adding collagen, 100 μL of media with collagen and cells (4×10^3/100 mL), were pipetted into each well. The plate was incubated at 37°C for 45 minutes to allow collagen to polymerize. Then, 150 μL of defined media (1:1 DMEM/F12 with ITS, 5×10^{-8} mol/L hydrocortisone, 5×10^{-5} mol/L triiodothyronine) containing 5 μmol/L of forskolin and 5 ng/mL of EGF was added on to the polymerized gel to initiate cyst growth. Following formation of cysts at day 4, the agonists (FSK and EGF) were removed and the gels were rinsed twice with defined media. To initiate drug treatments, Quinomycin A at different concentrations was added to the wells with media. Fresh treatment media with drug was replaced every day for each treatment. After 4 days, the outer diameter of cross-sectional images of spherical cysts with distinct lumens were measured using a digital camera attached to an inverted microscope and analyzed with video analysis software (Image Pro-Premier, Media Cybernetics). Surface area was calculated from the outer diameters and total surface area of the cysts was determined from the sum of individual cysts within each well (6 wells per treatment). Cysts with diameters of 50 μmol/L or less were excluded. Data are presented as surface area/mm^2.

2.8 | Immunohistochemistry/immunofluorescence

IHC was performed as described previously.[24] Briefly, kidney sections from wild-type and PKD mice treated with Quinomycin A (quin) or vehicle (veh) were deparaffinized with xylene and hydrated with graded ethanol. Sections were then boiled in citrate buffer (10 mmol/L of sodium citrate, 0.05% Tween 20, pH: 6.0) and cooled to room temperature.

Sections were incubated for 30 minutes with 3% hydrogen peroxide for IHC or 0.5 mol/L ammonium chloride for IF to block endogenous peroxidase or fluorescence activity, respectively. Subsequent washing in PBS and blocking with 10% normal serum (in PBS from the species the secondary antibody was raised in) for 1 hour were followed by incubation for 1 hour with primary antibodies in a humidified chamber. Slides were washed in PBS and incubated for 1 hour in 1:400 diluted biotin-conjugated secondary antibodies (Vector Laboratories) for IHC and 1:400 Alexa Fluor 488 or Alexa Fluor 594 (Invitrogen, Thermo Fisher Scientific) for IF. For DBA and LTA staining, slides were incubated with 1:500 dilution of each followed by washing with PBS. For IF, the slides were cover slipped using Prolong Diamond Antifade (Invitrogen, Thermo Fisher Scientific) and sealed with clear nail polish. For IHC, the slides were further incubated with avidin-biotin-peroxidase complex (ABC Elite; Vector Laboratories) and detected with diaminobenzidine (DAB; Sigma-Aldrich). Tissue sections for IHC were then dehydrated with graded ethanol and mounted with permount before coverslipping (Thermo Fisher Scientific). Slides were visualized and imaged using a Nikon 80i microscope with a photometrics camera or a Nikon Eclipse TiE attached to an A1R-SHR confocal, with an A1-DU4 detector, and LU4 laser launch.

For quantification of cell proliferation, Ki67-labeled sections were counterstained with hematoxylin to visualize the nucleus. Images were acquired from four random fields from each mouse section (total four mice in each group) and the total number of nuclei and Ki67-positive cells were counted in a blinded fashion. Data from each field were averaged and presented as percent Ki67-positive cells.

Cilia length quantification: Tissue sections immunostained for acetylated α-tubulin and DBA were imaged at multiple planes, which were then merged to obtain full-length cilia. Cilia images were converted to black and white and cilia lengths were quantified using ImageJ.

2.9 | Western blots

Following treatments, cells were washed with PBS three times and lysed. Tissues (fresh or frozen) were chopped in pieces and homogenized using a Dounce homogenizer. For both cells and tissues, RIPA lysis buffer (50 mmol/L of Tris HCl pH7.5, 137 mmol/L of NaCl, 1% of IGEPAL, and 2 mmol/L of EDTA) with protease inhibitors (Halt Protease inhibitor Cocktail, Thermo Fisher Scientific) was used.[9] Protein concentration was measured using Bio-Rad DC protein Assay kit (Bio-Rad). Whole-cell lysates (50 to 100 µg) were solubilized in 6X Laemmli sample buffer and heated to 95°C for 10 minutes and electrophoresed on 15% or 10% polyacrylamide gels. Proteins were transferred to PVDF membranes. Ponceau staining was performed for each blot to determine protein transfer and imaged. Ponceau S represented total protein and was used to normalize the gels for protein loading.[25] The immunoblots were blocked in 5% nonfat dry milk in PBST (PBS containing 0.1% Tween 20) for 1 hour at room temperature and then, followed by PBS washes; the blots were incubated with appropriate dilutions of primary antibodies overnight. The blots were then washed and incubated with secondary antibodies (1:10,000 dilution in blocking solution) for 1 hour at room temperature. After subsequent washes in PBST, bound antibody was detected by chemiluminescence (Western Lightning Plus ECL, Perkin Elmer). Bands produced in the results were quantified using ImageJ and normalized with Ponceau S staining to confirm equal loading.[25] Data were presented as relative intensity.

2.10 | Apoptosis

Apoptosis was evaluated in tissue sections obtained from vehicle and Quinomycin A-treated PKD mice using "In situ Apoptosis detection kit" obtained from Abcam. Manufacturer's instructions were followed.

2.11 | Statistics

Data are expressed as mean ± SE. Statistical significance was measured by Student's unpaired *t* test for comparison between control and PKD groups. One-way ANOVA was performed to compare more than two groups followed by the Tukey's HSD test. A $P < .05$ was considered statistically significant.

3 | RESULTS

3.1 | Quinomycin A treatment reduces cyst growth of human ADPKD cells cultured within 3D collagen gels

Studies have shown that Quinomycin A is an anticancer agent that intercalates double-stranded DNA. As low as 5 nmol/L Quinomycin A was able to induce cell cycle arrest in pancreatic cancer cells.[14] We first determined the effects of Quinomycin A on kidney cell viability. Normal human kidney (NHK) cells and ADPKD cells obtained from cortical cysts of ADPKD patients were treated with increasing concentrations of Quinomycin A starting from 0.3 to 10 nmol/L (Figure 1A). Treatments were continued for four consecutive days. Quinomycin A was well tolerated by both NHK and ADPKD cells at concentrations below 2 nmol/L. With increasing concentrations thereafter, percent viability of ADPKD cells declined. By 10 nmol/L, the viability of

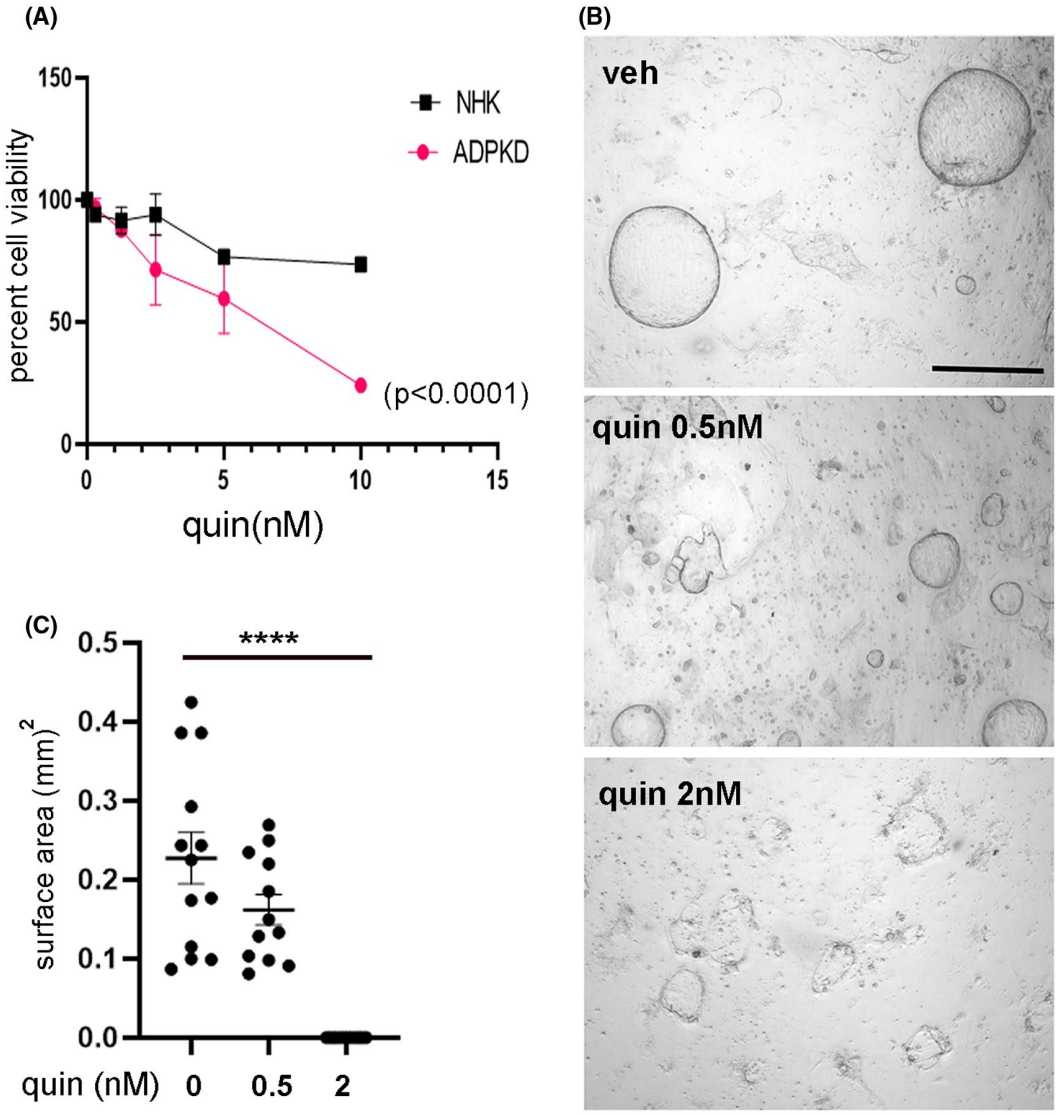

FIGURE 1 Primary human ADPKD cells are sensitive to Quinomycin A treatments. A, Primary cells from normal human kidney (NHK) and ADPKD cysts (n = 3-5) at each data point were cultured in the presence of Quinomycin A for 4 days followed by viability assays. Data are presented as percent viability. B, Primary ADPKD cells were grown to form cysts on a three-dimensional (3D) system using collagen matrix in the presence of forskolin and EGF for 3-5 days followed by treatment with vehicle or Quinomycin A (quin) for four additional days. Cysts were fixed, imaged, and measured. C, Cyst size represented as surface area from an ADPKD patient (six or more replicates/treatment). Each point represents a replicate. Statistical significance was determined by multiple unpaired *t* tests for panel A and one-way ANOVA followed by Tukey's multiple comparison test (****$P < .0001$). Scale bar: 0.57 mm

NHK cells dropped 73.8%, whereas ADPKD cells dropped their viability to 24%. The dose response curve showed that ADPKD cells are more sensitive to Quinomycin A. We next performed 3D cyst assays using primary ADPKD renal epithelial cells[21] to examine the potential of Quinomycin A to inhibit cyst growth. ADPKD cells were induced to form cysts in a collagen gel in the presence of the cAMP agonist FSK and growth factor EGF. After cyst formation, Quinomycin A at desired concentrations was used for four consecutive days and the effects on cyst progression were evaluated. As shown in Figure 1B,C, Quinomycin A reduced the size of in vitro cysts, relative to vehicle treatment. Of note, while treatment with 2 nmol/L Quinomycin A resulted in only a 20% viability loss of ADPKD cells grown in 2D (Figure 1A), the same treatment of Quinomycin A obliterated cysts when cells were grown in 3D (Figure 1B,C). These data suggest that cysts may intrinsically be more dose-sensitive than cells grown in 2D.

3.2 | Quinomycin A inhibits cyst progression in a PKD mouse model

We next examined the effects of Quinomycin A in an orthologous mouse model of ADPKD. We generated $Pkd1^{RC/RC}$; $Pkd2^{+/-}$ mice by breeding $Pkd1^{RC/RC}$ mice

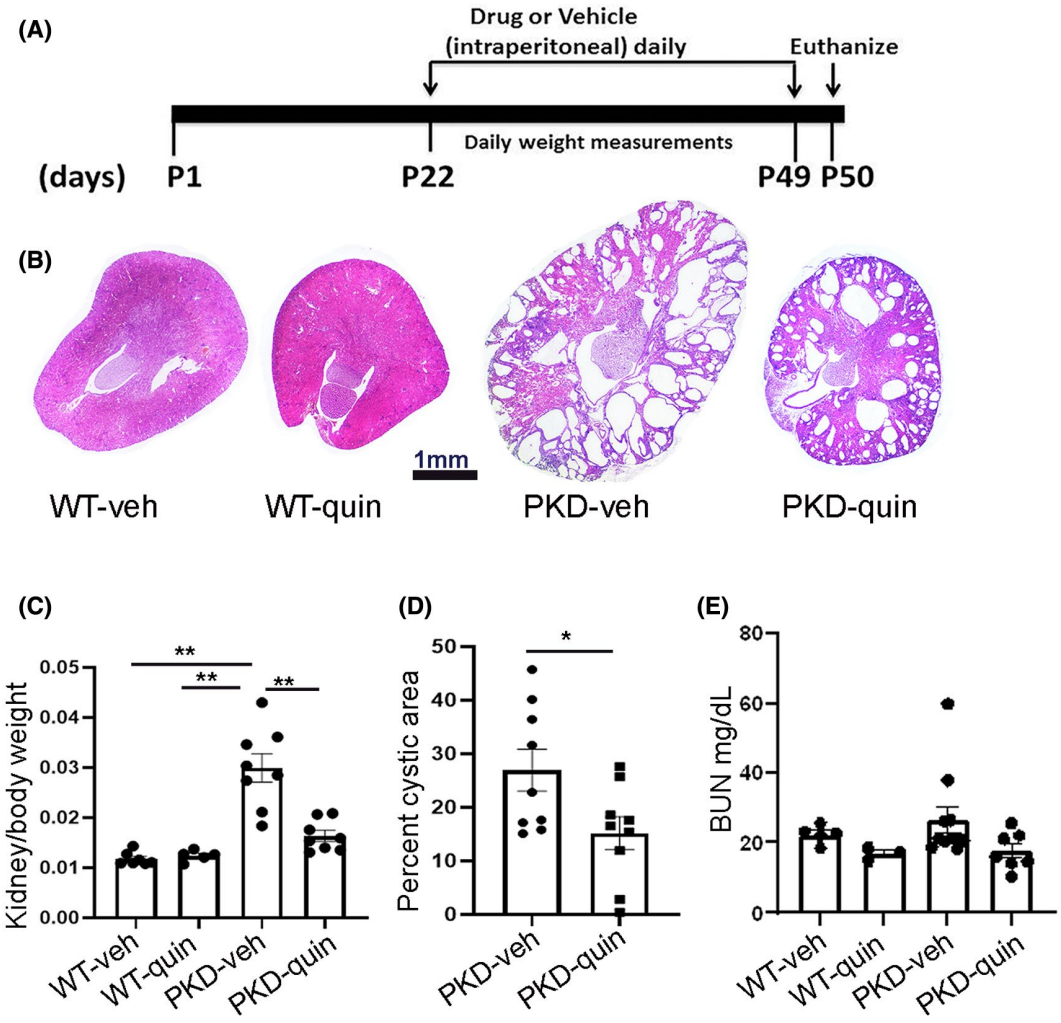

FIGURE 2 Quinomycin A reduces disease progression in a mouse model of ADPKD. A, Experimental timeline for Quinomycin A treatments. PKD or WT mice (postnatal day 22) were intraperitoneally injected with vehicle (veh) or Quinomycin A (10 mg/kg body weight) for 27 consecutive days. B, H&E staining of kidney sections. Representative images of each treatment group are shown. C, Total kidney to body weight ratio of vehicle and Quinomycin A-treated PKD and WT mice. D, Cystic index of PKD kidneys measured as percent cystic area. E, Serum urea nitrogen values measured as mg/dL. Each dot represents a mouse in C through E. Data are presented as mean ± SE (n = 4-8 per group). Statistical significance was determined using unpaired Student's *t* test (D) or one-way ANOVA followed by Tukey's HSD test (*$P < .05$), (**$P < .01$). Scale bar: 1 mm

with *Pkd2*$^{+/-}$ mice (both on a C57BL/6J background)[15,16] (Figure S1A). Homozygous *Pkd1*$^{RC/RC}$ mice have a slow progressing cyst phenotype, while heterozygous *Pkd2*$^{+/-}$ have no phenotype. However, when these mice are bred to obtain *Pkd1*$^{RC/RC}$; *Pkd2*$^{+/-}$ mice, cyst formation is accelerated. In contrast to *Pkd1*$^{RC/RC}$ mice, total kidney weight (KW) (% body weight, BW) of *Pkd1*$^{RC/RC}$; *Pkd2*$^{+/-}$ mice progressively increased during the first 5 weeks after which changes in KW (%BW) were similar to those of *Pkd1*$^{RC/RC}$ mice (Figure S1A). Cyst surface area (cystic index) was measured in *Pkd1*$^{RC/RC}$; *Pkd2*$^{+/-}$ mice at week 1, 3, and 4, the time period when there is rapid increase of KW (%BW). The data showed progressively growing cysts which increased in size from week 1 to week 4 (Figure S1B). We selected a time point of 3 weeks for our studies when cysts were actively growing in *Pkd1*$^{RC/RC}$; *Pkd2*$^{+/-}$ mice (hereafter called PKD mice). In previous studies, Quinomycin A concentration of 10 µg/kg body weight by daily intraperitoneal injections for up to 200 days did not result in any adverse effects.[13] Based on these studies, PKD and littermate wild-type (WT) control mice were weaned at P21 and daily intraperitoneal injections of Quinomycin A (10 µg/kg body weight) were administered from P22-P49. Mice were euthanized at P50, and tissues and blood samples were collected (Figure 2A). Kidneys of vehicle- and Quinomycin A-treated WT mice appeared similar (Figure S2). In contrast, a reduction in kidney size (Figure 2B) was observed in Quinomycin A-treated PKD kidneys compared to vehicle-treated PKD kidneys. As expected, the kidney size correlated with kidney-to-body weight ratios (Figure 2C),

showing a significant reduction ($P < .05$) in Quinomycin A-treated PKD mice relative to vehicle-treated PKD mice. This correlated with a significant reduction in cystic area in the Quinomycin A-treated PKD group in comparison to the vehicle-treated PKD group (Figure 2D) (Figure S2). Renal function, as assessed by BUN levels, was not statistically different among the groups, however there was a trend for a decrease in BUN in PKD mice receiving Quinomycin A compared to vehicle (Figure 2E). These data indicate that Quinomycin A provides therapeutic benefit against PKD progression.

3.3 | Quinomycin A reduces cell proliferation and increases apoptosis in cyst lining epithelia

The DNA intercalating functions of Quinomycin A affects dividing cells. We asked whether Quinomycin A can block cell proliferation, a hallmark of PKD. Kidneys from control and PKD mice were labeled for Ki67, a proliferation marker. Serial sections were also labeled for DBA and LTA to identify the collecting ducts (CD) and proximal tubules (PT), respectively (Figure 3A). Vehicle-treated PKD mice exhibited $9.5 \pm 0.65\%$ positive cells for Ki67/ kidney section, whereas Quinomycin A-treated PKD mice showed a significant reduction with only $4.8\% \pm 0.86\%$ ($P < .007$) Ki67-positive cells on immunolabeling (Figure 3A,B). Cyst epithelial as well as interstitial cells stained positive for Ki67, we quantified percent Ki67-positive cells in DBA and LTA tubular compartments. In PKD sections, LTA- and DBA-positive cyst lining segments expressed similar percent of Ki67-positive cells, 17.82 ± 2.23 and 18.39 ± 1.9, respectively, which reduced to $9.7 \pm 1.9\%$ and $4.7 \pm 2.3\%$, respectively, after Quinomycin A treatment (Figure 3A,C,D). The data show that cystic epithelial cells of both collecting duct and proximal tubule origin contributed to majority of Ki67-positive cells in PKD mice, which reduced upon Quinomycin A treatment. Since ADPKD cells were sensitive to Quinomycin A (Figure 1), we performed TUNEL labeling to determine the apoptosis status in Quinomycin A-treated WT and PKD mice. As shown in Figure 3E,F, PKD mice exhibited mild apoptosis in cystic epithelium (arrows) ($1.9\% \pm 0.65\%$ TUNEL-positive cells) which significantly increased in Quinomycin A treatments (7.5 ± 2.29) ($P < .008$) showing that Quinomycin induces apoptosis in cystic epithelia.

3.4 | Quinomycin A reduces smooth muscle actin in PKD

We immunolabeled the sections for presence of the myofibroblast marker, alpha smooth muscle actin (α-SMA) which is normally expressed in smooth muscle cells (SMCs) surrounding blood vessels. PKD kidneys were highly positive for α-SMA labeling present around cysts (Figure 4A). In contrast to vehicle-treated PKD kidneys, Quinomycin A treatment in PKD mice reduced α-SMA labeling (Figure 4A,B). SMA expression was increased in areas around both DBA- and LTA-positive cysts. Quinomycin treatment reduced SMA staining regardless of the cyst origin. (Figure 4A,B). Western blot analyses of kidney lysates from Quinomycin A- and vehicle-treated WT and PKD mice (Figure 4C) showed low expression of α-SMA in Quinomycin A- and vehicle-treated WT kidneys, but a marked increase ($P < .001$) of α-SMA was observed in PKD (veh) kidneys. In contrast, Quinomycin A treatment significantly decreased α-SMA expression to levels comparable to control. These data show that Quinomycin A partially rescues PKD progression by decreasing myofibrotic activity which also reflects less fibrosis.

3.5 | Quinomycin A treatment inhibits Notch signaling in ADPKD mice

We previously reported that the Notch signaling pathway is activated in cyst-lining epithelial cells and interstitial cells of mouse PKD models and in human ADPKD tissue and primary cultures of cystic cells.[9] Since Quinomycin A can target the Notch signaling pathway,[14] we examined whether Quinomycin A can affect Notch signaling pathway in our model. IHC for Notch3 revealed reduced Notch3 labeling, especially in the cystic epithelial cells (Figure 5A, arrows). Western blots revealed that there was a decreasing trend in Notch3 IC protein following Quinomycin A treatment in PKD mice, it did not reach significance (Figure 5B). However, other members of the Notch pathway, RBPjk,and HeyL which were significantly elevated in PKD lysates (Figure 5C,D), showed a significant reduction in kidneys treated with Quinomycin A. Our data show that Quinomycin A effectively targets the Notch signaling and protects mice from kidney injury.

3.6 | Quinomycin A normalizes cilia length in an ADPKD mouse model

Studies have shown that cilia are lengthened in kidney epithelial cells of PKD mouse models, which may reflect defects in ciliary homeostasis.[15,26-28] Thus, we assessed the effect of Quinomycin A on cilia length in mouse kidneys. Kidney sections were immunolabeled for the presence of acetylated α-tubulin which marks cilia and for DBA lectin which stains collecting ducts, where cysts predominantly develop in ADPKD. Immunofluorescence (IF) labeling revealed that cilia were lengthened in vehicle-treated PKD kidneys compared to the vehicle-treated WT kidneys (Figure 6A) and that

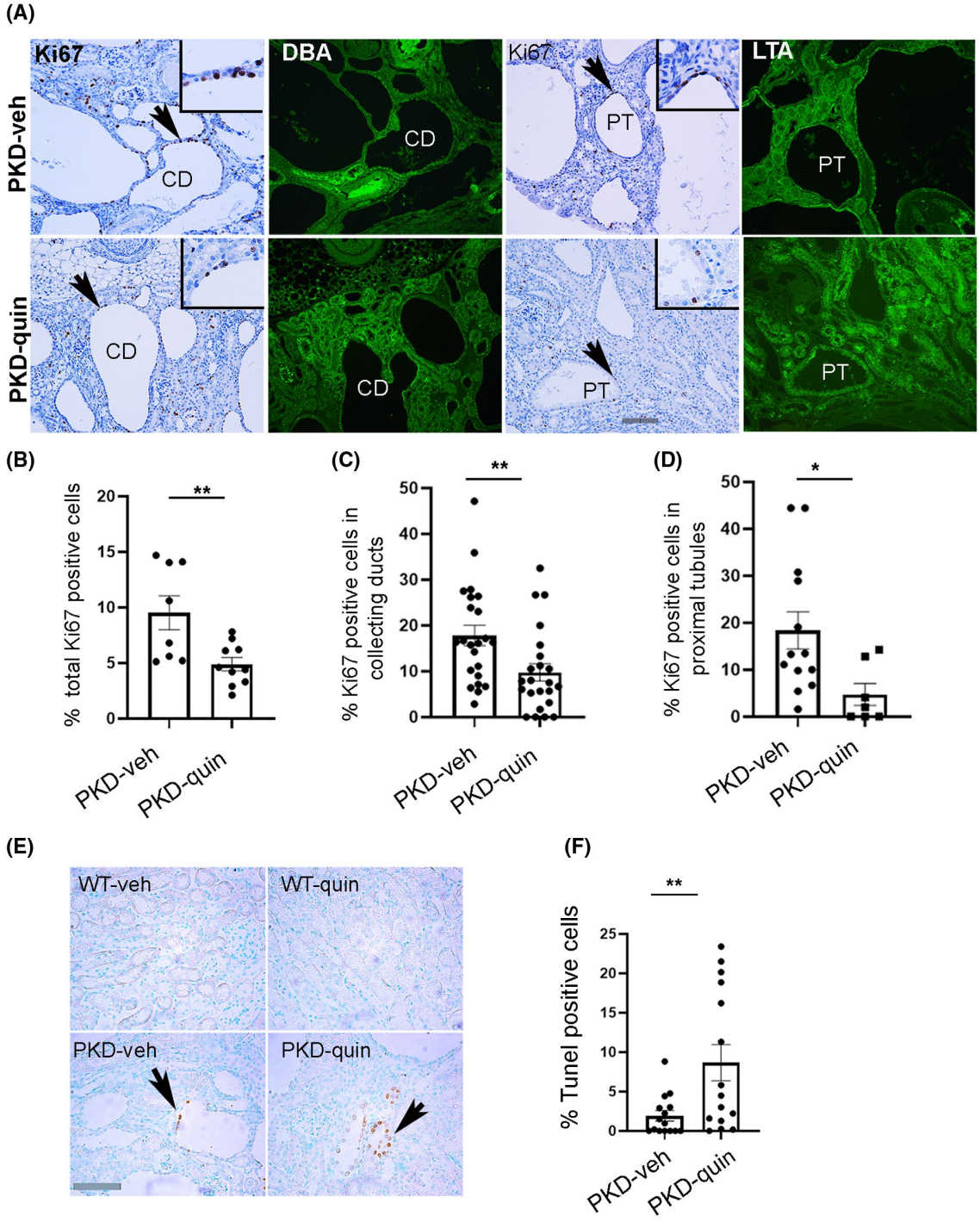

FIGURE 3 Quinomycin A slows cell proliferation and myofibrosis in PKD. A, Ki67 staining was performed by Immunohistochemistry (IHC) to assess cell proliferation in Quinomycin A- and vehicle-treated PKD kidneys. Serial sections were also labeled for *Dolichos biflorus* agglutinin (DBA) to identify collecting ducts (CD) and *Lotus tetragonolobus* agglutinin (LTA) to identify proximal tubules (PT) using IF. Arrows point to proliferative areas, which are also presented as insets in Ki67-labeled panels. Hematoxylin staining shows blue nuclei and Ki67-positive nuclei are shown in dark brown. B, Quantification of Ki67 staining expressed as percent total Ki67-positive cells from at least 7 to 10 images randomly taken from 4 mice in each group. C, Quantification of Ki67 cells from DBA-positive cystic segments showing collecting duct-positive cells. D, Quantification of Ki67 cells from LTA-positive cystic segments showing proximal tubule-positive cells. Each point in C and D refers to DBA- or LTA-positive cyst expressing Ki67. E, TUNEL staining was performed to identify cells undergoing apoptosis in WT and PKD kidneys treated with vehicle or Quinomycin A. Blue cells reflect nuclei and brown cells (arrows) identify cells undergoing apoptosis. F, Apoptosis was quantified as percent TUNEL-positive cells in 15 sections from 4 different mice in each group. Unpaired Student's *t* test used for statistical analysis. Data are presented as mean ± SE, (**P* < .05), (***P* < .01). Scale bar: 100 μm

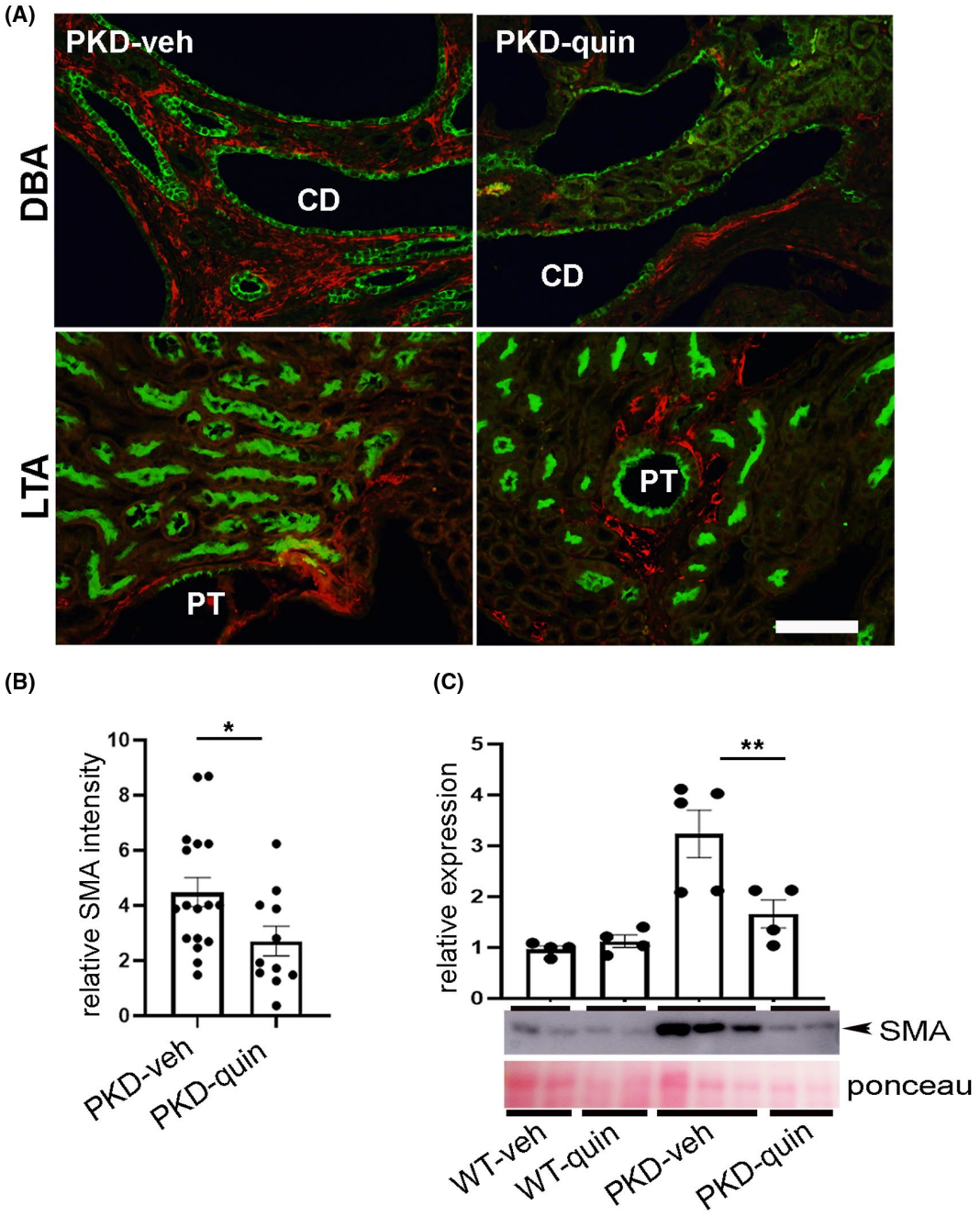

FIGURE 4 Quinomycin A treatment decreases smooth muscle actin in PKD. A, Double IF staining was performed to detect smooth muscle actin (SMA) accumulation (red) along with DBA or LTA (green) in mice treated with vehicle or Quinomycin A. B, Total intensity of SMA was quantified in images from vehicle (n = 17) and Quinomycin A (n = 11)-treated PKD mice (n = 4 each). C, Western blots were performed in lysates from Quinomycin A-treated WT or PKD mice for detection of SMA. Band intensities were quantified and normalized against Ponceau S expression and presented as relative expression. Unpaired Student's *t* test (A) and one ANOVA followed by Tukey's HSD test was used for statistical analysis. Data are presented as mean ± SE, (*$P < .05$), (**$P < .01$). Scale bar: 100 μm

Quinomycin A treatments shortened cilia lengths in PKD kidneys (Figure 6A, arrows, magnified insets under each image). Quantification of cilia length within kidneys confirmed that there was a highly significant ($P < .0001$) cilia length reduction following Quinomycin A treatment in PKD mice, indicating that Quinomycin A restores cilia lengths in a PKD mouse model (Figure 6B).

4 | DISCUSSION

In this study, we show that Quinomycin A effectively reduces in vitro cyst growth of primary cyst epithelial cells obtained from ADPKD patients. We also show that normal human kidney epithelial cells are less sensitive to Quinomycin A than ADPKD cells, indicating that Quinomycin A can spare

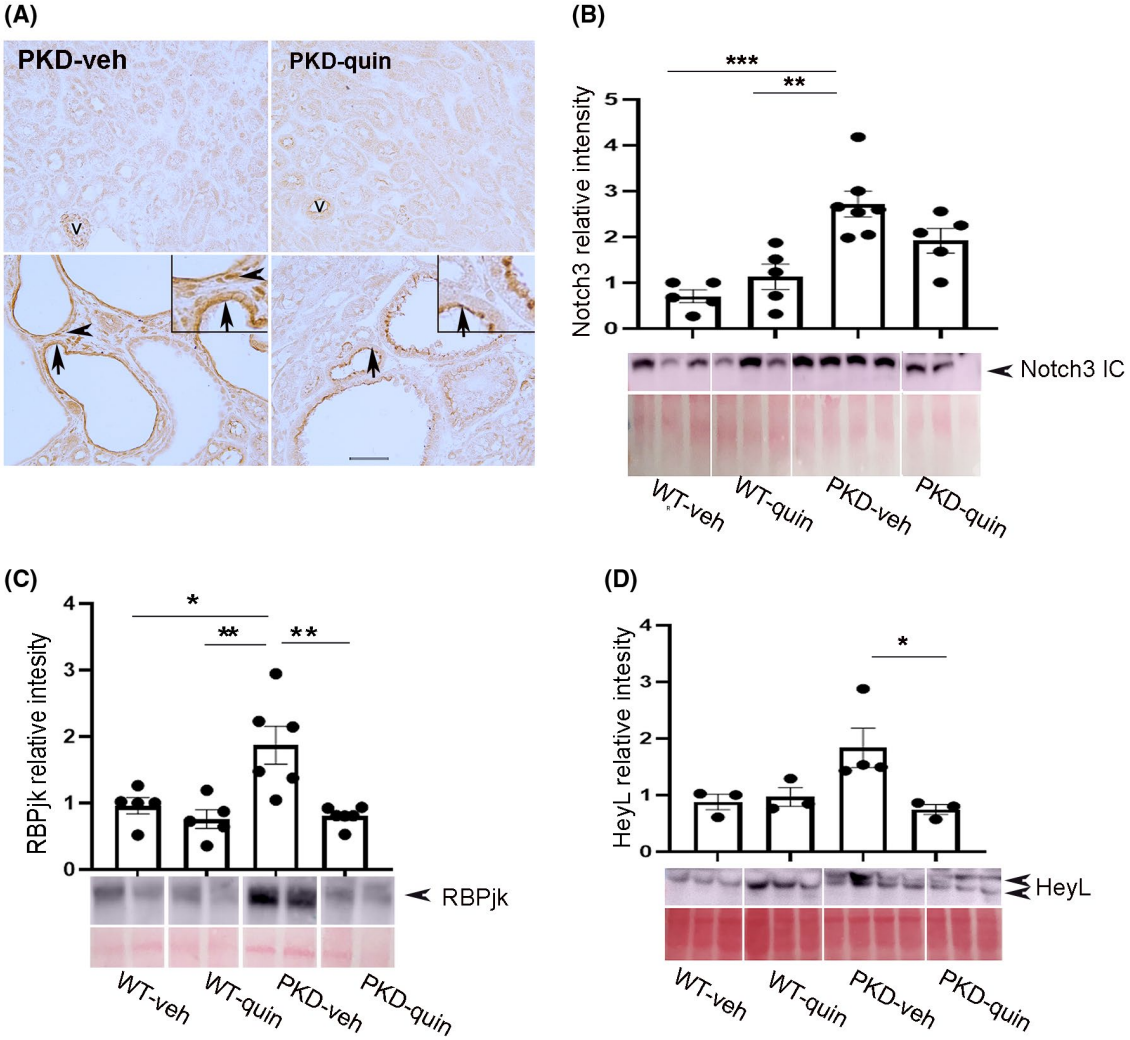

FIGURE 5 Quinomycin A targets the Notch signaling pathway in PKD. A, Immunohistochemistry (IHC) for Notch3. B, Western blot (WB) analysis for Notch3 IC and cumulative quantitative data (C and D) Western blot analysis for RBPjk and HeyL showing increased expression in kidney lysates of vehicle-treated PKD mice and that Quinomycin A treatments reducing this expression. Protein blots were quantified using Ponceau S staining for total protein normalization. Data are presented as relative change. Each dot represents an individual mouse. Data are presented as mean ± SE. Statistical significance was determined using one-way ANOVA followed by Tukey's HSD test (*$P < .05$), (**$P < .01$), (***$P < .001$). Scale bar: 100 μm

normal epithelial cells, while targeting the cystic cells. In support of our study, in vitro studies have been performed with concentrations of Quinomycin A as low as 5 nmol/L in several cancerous cell lines.[29,30] In pancreatic cell lines this concentration inhibited cancer cell proliferation but did not affect normal pancreatic ductal epithelial cells even at a concentration of 50 nmol/L, supporting our observation that normal cells are less responsive to Quinomycin A. The data are further supported by the 3D in vitro cyst assays in which ADPKD cells grown as cysts were responsive to even lower doses of Quinomycin A than ADPKD cells grown in 2D. This effect could be attributed to dependence of cyst formation on cAMP. While cell viability is tested in cells grown in media without addition of other signaling factors, initiation of cyst formation in vitro (3D) takes place in response to forskolin, an agonist of cyclic AMP, an important mediator of cyst progression.[21,31] Thus, it is possible that Quinomycin A sensitivity is associated with increased cAMP signaling. Further studies will be required to support this observation.

Quinomycin A is a member of quinoxaline family of antibiotics previously identified as an anticancer drug that binds strongly to double-stranded DNA.[12] Due to its strong DNA chelator property, Quinomycin A can be harmful in high doses and prior clinical trials have documented multiple toxicities resulting in drug development being halted. These toxicities were attributed to the higher dose of 180 mg/m^2 of Quinomycin A.[32-38] Doses of 60-120 mg/m^2 were found to have no toxicity.[39] Recent studies in mice indicate that low doses (eg, 10 μg/kg body weight) of Quinomycin A are not toxic to normal cell hematopoiesis and selectively targets cancerous cells in acute myelocytic leukemia and bladder cancer.[13,14] To further combat the

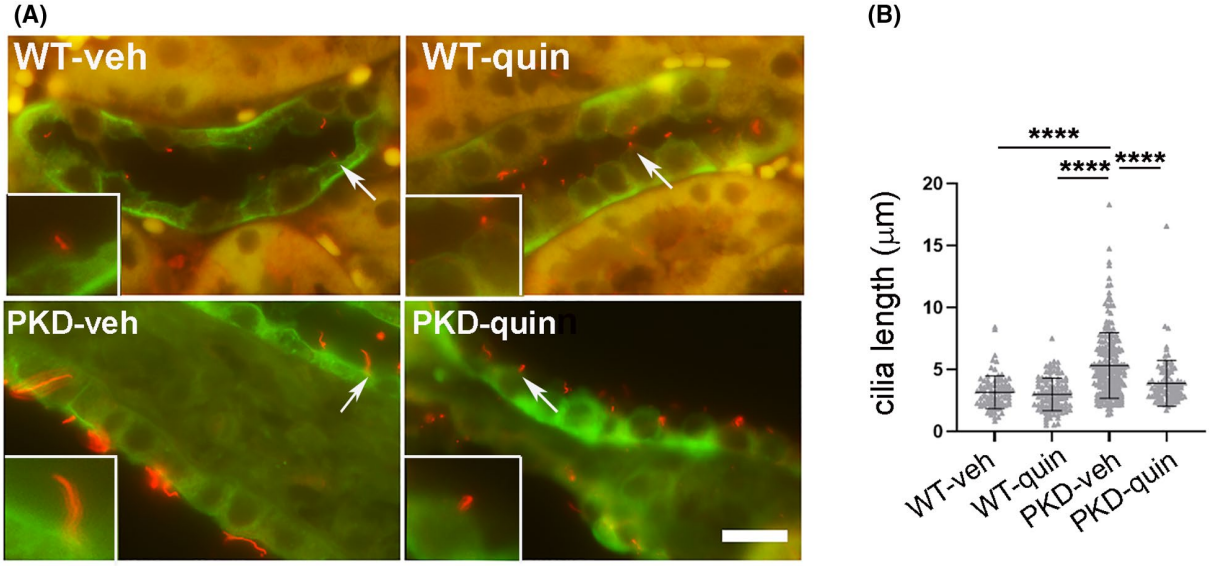

FIGURE 6 Quinomycin A normalizes cilia length in PKD kidneys. A, Double immunostaining of primary cilia marker protein, acetylated tubulin (red) together with *Dolichos biflorus agglutinin* (DBA)(green). Arrows represent cilium that is magnified and shown in insets. B, Cilia length was quantified from n = 4 mice per group. Each data point represents a cilium. Data are presented as mean ± SE. Statistical significance was determined using one-way ANOVA followed by Tukey's HSD test ($P < .0001$). Scale bar: 10 μm

negative effects of Quinomycin A, a recent study showed that actively targeted nano-delivery of Quinomycin A can efficiently target cancer cells to induce autophagic cell death instead of apoptosis or necrotic cell death.[40] In our studies, we found that ADPKD cells lose significant viability at a higher dose of 10 nmol/L Quinomycin A whereas, NHK cells retain their viability. Our in vitro studies also indicated that Quinomycin A specifically targeted cystic epithelial cells for apoptosis. Since PKD is a genetic disease and may require life-long treatment, it is plausible that Quinomycin A may show toxic effects in that scenario. We speculate that alternate treatments of Tolvaptan together with targeted nano-delivery of Quinomycin A may have better prognosis for which further studies are required.

In addition to targeting the Notch pathway, Quinomycin A has been shown to target HIF-1α. HIF-1α expression is increased in cystic epithelia and was found to be associated with increased cyst growth by activating fluid secretion.[41] We have previously shown Notch3 activation in cyst lining and interstitial cells in PKD.[9] It is possible that cross talk between HIF-1α and Notch signaling exists in cystic tissues as documented previously where HIF-1α binds to cleaved Notch resulting in stabilization and activation of Notch signaling.[42,43] In another study, chronic hypoxia was shown to activate Notch signaling in prostate cancer. Although we were not successful in detecting HIF-1α in the kidney nuclear extracts of the PKD mice by Western blottings or IHC, Quinomycin A reduced the Notch pathway downstream members, RBPjk and HeyL. The Notch pathway is increased in cyst lining epithelia, and the signal is attenuated in the presence of Quinomycin A. Whether the relationship is direct and Quinomycin A is modulating the Notch pathway via a direct inhibition or by inhibiting other processes that impact the latter remains to be determined.

Elongation of cilia has been observed on tubular epithelial cells in PKD.[26,27] The primary cilium is an antenna-like mechano- and chemosensor that detects fluid flow and transduces extracellular signals into the cells in order to maintain renal function and nephron structure.[44,45] Several studies have suggested that cilia elongation can be a critical factor in conferring kidney disease resistance.[46,47] Moreover, Notch activation leads to lengthening of cilia in the developing neural tube in mouse embryos and in NIH3T3 cells.[48] Thus, it is possible that Quinomycin A reduces Notch signaling, which in turn, results in shortening of cilia in PKD kidneys in our mouse model. This hypothesis will need further evaluation.

Taken together, we show that Quinomycin A inhibits the Notch signaling pathway, reduces cilia length, and confers protection against cyst progression in ADPKD by reducing cellular proliferation and fibrosis, and inducing apoptosis in cyst lining epithelial cells. To the best of our knowledge, this is the first evidence in which Quinomycin A has been shown to alter cilia length and reduce renal cystic disease. The study adds Quinomycin A to the list of potential repurposed drugs that may prove beneficial to PKD patients.

ACKNOWLEDGMENTS

The authors thank Dr Rajni Vaid Puri, Sireesha Yerrathota, Johnny Dinh Phan, Francis Franco, and Anh Dao Do for technical assistance; Gail Reif and Yan Zhang for help with NHK and ADPKD cell preparation. Jing Huang in the KUMC histology core for sectioning of the kidneys. The Jared Grantham

Kidney Institute PKD Rodent Model and Drug-Testing Core, supported by NIH/NIDDK U54DK126126, provided the Pkd1RC/RC;Pkd2183/+ mice.

COMPETING INTERESTS

The authors declare no competing or financial interests.

AUTHOR CONTRIBUTIONS

M.S conceived and designed the study. MS, PSR, MMT, JYI, WW, and BMc conducted experiments, PVT and DPW provided reagents. MS, DS, PVT, DPW, and JPC analyzed data and interpreted results of experiments, MS prepared figures; MS drafted the manuscript; MS, PVT, MMT, DS, DPW, and JPC edited and revised the manuscript; MS approved the final version of manuscript. All authors read and approved the final manuscript.

ORCID

Dharmalingam Subramaniam https://orcid.org/0000-0002-2710-485X
Pamela V. Tran https://orcid.org/0000-0003-4619-4376
James P. Calvet https://orcid.org/0000-0001-5928-9820
Darren P. Wallace https://orcid.org/0000-0003-4616-7669
Madhulika Sharma https://orcid.org/0000-0001-7488-5444

REFERENCES

1. Gallagher AR, Germino GG, Somlo S. Molecular advances in autosomal dominant polycystic kidney disease. *Adv Chronic Kidney Dis*. 2010;17(2):118-130.
2. Harris PC, Torres VE. Polycystic kidney disease. *Annu Rev Med*. 2009;60:321-337.
3. Nauli SM, Alenghat FJ, Luo Y, et al. Polycystins 1 and 2 mediate mechanosensation in the primary cilium of kidney cells. *Nature Genet*. 2003;33(2):129-137.
4. Torres VE, Chapman AB, Devuyst O, et al. Tolvaptan in patients with autosomal dominant polycystic kidney disease. *N Engl J Med*. 2012;367(25):2704-2718.
5. Reif GA, Yamaguchi T, Nivens E, Fujiki H, Pinto CS, Wallace DP. Tolvaptan inhibits ERK-dependent cell proliferation, Cl- secretion, and in vitro cyst growth of human ADPKD cells stimulated by vasopressin. *Am J Physiol Renal Physiol*. 2011;301(5):F1005-F1013.
6. Sorohan BM, Ismail G, Andronesi A, et al. A single-arm pilot study of metformin in patients with autosomal dominant polycystic kidney disease. *BMC Nephrol*. 2019;20(1):276.
7. Sweeney WE, Frost P, Avner ED. Tesevatinib ameliorates progression of polycystic kidney disease in rodent models of autosomal recessive polycystic kidney disease. *World J Nephrol*. 2017;6(4):188-200.
8. Zhou X, Fan LX, Sweeney WE Jr, Denu JM, Avner ED, Li X. Sirtuin 1 inhibition delays cyst formation in autosomal-dominant polycystic kidney disease. *J Clin Invest*. 2013;123(7):3084-3098.
9. Idowu J, Home T, Patel N, et al. Aberrant regulation of Notch3 signaling pathway in polycystic kidney disease. *Scient Rep*. 2018;8(1):3340.
10. Ran Y, Hossain F, Pannuti A, et al. γ-Secretase inhibitors in cancer clinical trials are pharmacologically and functionally distinct. *EMBO Mol Med*. 2017;9(7):950-966.
11. Foster BJ, Clagett-Carr K, Shoemaker DD, et al. Echinomycin: the first bifunctional intercalating agent in clinical trials. *Investig New Drugs*. 1985;3(4):403-410.
12. Waring MJ, Wakelin LP. Echinomycin: a bifunctional intercalating antibiotic. *Nature*. 1974;252(5485):653-657.
13. Wang Y, Liu Y, Tang F, et al. Echinomycin protects mice against relapsed acute myeloid leukemia without adverse effect on hematopoietic stem cells. *Blood*. 2014;124(7):1127-1135.
14. Ponnurangam S, Dandawate PR, Dhar A, et al. Quinomycin A targets Notch signaling pathway in pancreatic cancer stem cells. *Oncotarget*. 2016;7(3):3217-3232.
15. Hopp K, Ward CJ, Hommerding CJ, et al. Functional polycystin-1 dosage governs autosomal dominant polycystic kidney disease severity. *J Clin Invest*. 2012;122(11):4257-4273.
16. Wu G, Markowitz GS, Li L, et al. Cardiac defects and renal failure in mice with targeted mutations in Pkd2. *Nat Genet*. 2000;24(1):75-78.
17. Sharma M, Callen S, Zhang D, Singhal PC, Vanden Heuvel GB, Buch S. Activation of Notch signaling pathway in HIV-associated nephropathy. *AIDS (London, England)*. 2010;24C(14):2161-2170.
18. Reif GA, Yamaguchi T, Nivens E, Fujiki H, Pinto CS, Wallace DP. Tolvaptan inhibits ERK-dependent cell proliferation, Cl(-) secretion, and in vitro cyst growth of human ADPKD cells stimulated by vasopressin. *Am J Physiol Renal Physiol*. 2011;301(5):F1005-F1013.
19. Yamaguchi T, Nagao S, Wallace DP, et al. Cyclic AMP activates B-Raf and ERK in cyst epithelial cells from autosomal-dominant polycystic kidneys. *Kidney Int*. 2003;63(6):1983-1994.
20. Reif GA, Wallace DP. ADPKD cell proliferation and Cl(-)-dependent fluid secretion. *Methods Cell Biol*. 2019;153:69-92.
21. Sharma M, Reif GA, Wallace DP. In vitro cyst formation of ADPKD cells. *Methods Cell Biol*. 2019;153:93-111.
22. Wallace DP, Grantham JJ, Sullivan LP. Chloride and fluid secretion by cultured human polycystic kidney cells. *Kidney Int*. 1996;50(4):1327-1336.
23. Reif GA, Yamaguchi T, Nivens E, Fujiki H, Pinto CS, Wallace DP. Tolvaptan inhibits ERK-dependent cell proliferation, Cl^- secretion, and in vitro cyst growth of human ADPKD cells stimulated by vasopressin. *Am J Physiol Renal Physiol*. 2011;301:F1005-F1013.
24. Sharma M, Magenheimer LK, Home T, et al. Inhibition of Notch pathway attenuates the progression of human immunodeficiency virus-associated nephropathy. *Am J Physiol Renal Physiol*. 2013;304(8):F1127-F1136.
25. Sander H, Wallace S, Plouse R, Tiwari S, Gomes AV. Ponceau S waste: Ponceau S staining for total protein normalization. *Anal Biochem*. 2019;575:44-53.
26. Husson H, Moreno S, Smith LA, et al. Reduction of ciliary length through pharmacologic or genetic inhibition of CDK5 attenuates polycystic kidney disease in a model of nephronophthisis. *Human Mol Genet*. 2016;25(11):2245-2255.
27. Gerakopoulos V, Ngo P, Tsiokas L. Loss of polycystins suppresses deciliation via the activation of the centrosomal integrity pathway. *Life Sci Alliance*. 2020;3(9):e202000750.
28. Shao L, El-Jouni W, Kong F, et al. Genetic reduction of cilium-length by targeting intraflagellar transport 88 protein impedes kidney and liver cysts formation in mouse models of autosomal polycystic kidney disease. *Kidney Int*. 2020;98(5):1225–1241.

29. Yonekura S, Itoh M, Okuhashi Y, et al. Effects of the HIF1 inhibitor, echinomycin, on growth and NOTCH signalling in leukaemia cells. *Anticancer Res*. 2013;33(8):3099-3103.
30. Kong D, Park EJ, Stephen AG, et al. Echinomycin, a small-molecule inhibitor of hypoxia-inducible factor-1 DNA-binding activity. *Cancer Res*. 2005;65(19):9047-9055.
31. Putnam WC, Swenson SM, Reif GA, Wallace DP, Helmkamp GM Jr, Grantham JJ. Identification of a forskolin-like molecule in human renal cysts. *J Am Soc Nephrol*. 2007;18(3):934-943.
32. Chang AY, Kim K, Boucher H, et al. A randomized phase II trial of echinomycin, trimetrexate, and cisplatin plus etoposide in patients with metastatic nonsmall cell lung carcinoma: an Eastern Cooperative Oncology Group Study (E1587). *Cancer*. 1998;82(2):292-230.
33. Gradishar WJ, Vogelzang NJ, Kilton LJ, et al. A phase II clinical trial of echinomycin in metastatic soft tissue sarcoma. An Illinois Cancer Center Study. *Invest New Drugs*. 1995;13(2):171-174.
34. Wadler S, Tenteromano L, Cazenave L, et al. Phase II trial of echinomycin in patients with advanced or recurrent colorectal cancer. *Cancer Chemother Pharmacol*. 1994;34(3):266-269.
35. Shevrin DH, Lad TE, Guinan P, et al. Phase II trial of echinomycin in advanced hormone-resistant prostate cancer. An Illinois Cancer Council study. *Invest New Drugs*. 1994;12(1):65-66.
36. Chang AY, Tu ZN, Bryan GT, Kirkwood JM, Oken MM, Trump DL. Phase II study of echinomycin in the treatment of renal cell carcinoma ECOG study E2885. *Invest New Drugs*. 1994;12(2):151-153.
37. Muss HB, Blessing JA, DuBeshter B. Echinomycin in recurrent and metastatic endometrial carcinoma. A phase II trial of the Gynecologic Oncology Group. *Am J Clin Oncol*. 1993;16(6):492-493.
38. Marshall ME, Wolf MK, Crawford ED, et al. Phase II trial of echinomycin for the treatment of advanced renal cell carcinoma. A Southwest Oncology Group study. *Invest New Drugs*. 1993;11(2-3):207-209.
39. Kuhn JG, Von Hoff DD, Hersh M, et al. Phase I trial of echinomycin (NSC 526417), a bifunctional intercalating agent, administered by 24-hour continuous infusion. *Eur J Cancer Clin Oncol*. 1989;25(5):797-803.
40. Thomas A, Samykutty A, Gomez-Gutierrez JG, et al. Actively targeted nanodelivery of echinomycin induces autophagy-mediated death in chemoresistant pancreatic cancer in vivo. *Cancers*. 2020;12(8):2279.
41. Buchholz B, Schley G, Faria D, et al. Hypoxia-inducible factor-1α causes renal cyst expansion through calcium-activated chloride secretion. *J Am Soc Nephrol*. 2014;25(3):465-474.
42. Gustafsson MV, Zheng X, Pereira T, et al. Hypoxia requires notch signaling to maintain the undifferentiated cell state. *Dev Cell*. 2005;9(5):617-628.
43. Wang Y, Liu Y, Malek SN, Zheng P, Liu Y. Targeting HIF1α eliminates cancer stem cells in hematological malignancies. *Cell Stem Cell*. 2011;8(4):399-411.
44. Praetorius HA, Spring KR. A physiological view of the primary cilium. *Ann Rev Physiol*. 2005;67:515-529.
45. Park KM. Can Tissue cilia lengths and urine cilia proteins be markers of kidney diseases? *Chonnam Med J*. 2018;54(2):83-89.
46. Verghese E, Zhuang J, Saiti D, Ricardo SD, Deane JA. In vitro investigation of renal epithelial injury suggests that primary cilium length is regulated by hypoxia-inducible mechanisms. *Cell Biol Int*. 2011;35(9):909-913.
47. Overgaard CE, Sanzone KM, Spiczka KS, Sheff DR, Sandra A, Yeaman C. Deciliation is associated with dramatic remodeling of epithelial cell junctions and surface domains. *Mol Biol Cell*. 2009;20(1):102-113.
48. Stasiulewicz M, Gray SD, Mastromina I, et al. A conserved role for Notch signaling in priming the cellular response to Shh through ciliary localisation of the key Shh transducer Smo. *Development (Cambridge, England)*. 2015;142(13):2291-2303.

SUPPORTING INFORMATION

Additional Supporting Information may be found online in the Supporting Information section.

How to cite this article: Radadiya PS, Thornton MM, Daniel EA, et al. Quinomycin A reduces cyst progression in polycystic kidney disease. *The FASEB Journal*. 2021;35:e21533. https://doi.org/10.1096/fj.202002490R